

## Tentative Blazar Candidate EP240709A Associated with 4FGL J0031.5–5648: NICER and Archival Multiwavelength Observations

MASON NG <sup>1,2,3</sup> JEREMY HARE <sup>4,5,6</sup> GAURAVA K. JAISAWAL <sup>7</sup> CHRISTIAN MALACARIA <sup>8</sup> CRAIG B. MARKWARDT <sup>4</sup> AND  
ANDREA SANNA <sup>9</sup>

<sup>1</sup>MIT Kavli Institute for Astrophysics and Space Research, Massachusetts Institute of Technology, Cambridge, MA 02139, USA

<sup>2</sup>Department of Physics, McGill University, 3600 rue University, Montréal, QC H3A 2T8, Canada

<sup>3</sup>Trottier Space Institute, McGill University, 3550 rue University, Montréal, QC H3A 2A7, Canada

<sup>4</sup>Astrophysics Science Division, NASA Goddard Space Flight Center, Greenbelt, MD 20771, USA

<sup>5</sup>Center for Research and Exploration in Space Science & Technology II (CRESSST II), NASA/GSFC, Greenbelt, MD 20771, USA

<sup>6</sup>The Catholic University of America, 620 Michigan Ave., N.E. Washington, DC 20064, USA

<sup>7</sup>DTU Space, Technical University of Denmark, Elektrovej 327-328, DK-2800 Lyngby, Denmark

<sup>8</sup>INAF Osservatorio Astronomico di Roma, Via Frascati 33, 00078 Monte Porzio Catone (RM), Italy

<sup>9</sup>Dipartimento di Fisica, Università degli Studi di Cagliari, SP Monserrato-Sestu km 0.7, I-09042 Monserrato, Italy

### ABSTRACT

We report on follow-up observations of the recently discovered transient by the Einstein Probe, EP240709A, with the Neutron star Interior Composition Explorer (NICER). We also incorporated archival multiwavelength survey data from the Neil Gehrels Swift Observatory (X-ray), Gaia (optical), the Fermi Gamma-ray Space Telescope (gamma-ray), and the Wide-field Infrared Survey Explorer (infrared) to distinguish between blazars and stellar systems. We suggest that EP240709A is likely an active blazar.

**Keywords:** Blazars (164) — Active galactic nuclei (16)

### 1. INTRODUCTION

EP240709A was first discovered by the Wide-field X-ray Telescope (WXT) aboard the Einstein Probe (EP; Yuan et al. 2022) on 2024 July 9 with a 0.5–4.0 keV unabsorbed flux of  $1.3_{-0.5}^{+0.6} \times 10^{-11} \text{ erg s}^{-1} \text{ cm}^{-2}$  (Liu et al. 2024). A follow-up 4 ks observation by the Follow-up X-ray Telescope (FXT) onboard EP on 2024 July 11 showed that the source did not exhibit significant variability (Liu et al. 2024). Finally, archival Swift/XRT and eROSITA observations suggested that EP240709A is likely associated with 4FGL J0031.5–5648, due to the overlapping X-ray localization regions (see Section 3.2) between Swift/XRT, eROSITA, and EP/FXT (Liu et al. 2024). In this article, we report on follow-up NICER X-ray observations and utilize multiwavelength survey data to constrain the possible nature of the source.

### 2. OBSERVATIONS

The Neutron Star Interior Composition Explorer (NICER) observed EP240709A from 2024 July 17 to 2024 July 26 (ObsIDs 720467010x) for a total filtered exposure of 10.4 ks. The data were processed with `nicer12` with the default filtering criteria from 2024-02-09\_V012A of the NICER Data Analysis Software (NICERDAS) available through HEASo`ft` 6.33. For our pulsation searches and aperiodic timing analysis, we corrected the photon arrival times to the Solar System barycenter with the JPL DE421 solar system ephemeris (Folkner et al. 2009) and with source coordinates R.A. = 7°8964, DEC. = –56°7787 (position error of 3.6′′) from the Living Swift XRT Point Source Catalogue (LSXPS; Evans et al. 2023).

We generated spectral products with the `nicer13-spect` pipeline, and rebinned the spectra with optimal binning (Kaastra & Bleeker 2016) and ensured 25 minimum counts per spectral bin. We utilized the `nibackgen3C50` model (Remillard et al. 2022) to describe the background. Since the background spectra dominated above 3 keV, we restricted the spectral fitting to

the 0.4–3.0 keV energy range. We did not use data from ObsID 7204670106 due to the short exposure (22 s). The source and background (sw model<sup>1</sup>) light curves were constructed with `nicer13-1c`.

### 3. RESULTS

#### 3.1. NICER

The light curve (see Figure 1 a) does not show significant flaring activity. Inspecting the light curve with finer time bins (1 s bins; not plotted), we did not see any variability that would suggest a transitional millisecond pulsar in the sub-luminous disk state (Papitto & de Martino 2022).

We searched for coherent pulsations with acceleration searches (Ransom et al. 2002) over each of the 24 good time intervals in the 0.4–3.0 keV band. Acceleration searches are most sensitive for time intervals  $T < P_{\text{orb}}/10$ , where  $T$  is the interval length and  $P_{\text{orb}}$  is the binary orbital period (Ransom et al. 2002). The minimum, maximum, and median interval lengths were 430 s, 22 s, and 1077 s, respectively. We did not see any significant signals. Given the relative faintness of the source (less than 4 c/s), we caution interpreting non-detections in short (less than 500 s) intervals. We also constructed the 0.4–3.0 keV averaged power spectrum with 128 s bins to search for quasi-periodic oscillations, but we found a power spectrum consistent with Poisson noise. We place upper limits on the sinusoidal amplitude of any pulsed signal at  $\sim 31\%$  at 1 Hz and  $\sim 35\%$  at 500 Hz using the formalism described in Vaughan et al. (1994).

The NICER spectra were well described by an absorbed power law (reduced  $\chi^2 \sim 1.0$  for  $\sim 35$  d.o.f.). The power law index,  $\Gamma$ , varied between 1.9 and 2.6, and the 0.4–3.0 keV unabsorbed flux varied between  $(3\text{--}9)\times 10^{-12}$  erg s<sup>-1</sup> cm<sup>-2</sup>, indicating a slight decrease from the flux level initially reported by the EP team (Liu et al. 2024). The spectral parameters are also shown in Figures 1 a), b), and c). We fixed  $n_H = 0.048 \times 10^{22}$  cm<sup>-2</sup>, an exposure time-weighted average value taken from initially fitting an absorbed power law to all spectra from the NICER observations (with  $n_H$  being free).

#### 3.2. Multiwavelength Counterparts

The initial discovery of EP240709A by the EP team associated it with 4FGL J0031.5–5648, an unassociated Fermi source. In Figures 1 d) and e), we plot the variability indices, curvature significances, as well as the curvature parameters and peak energies (MeV) for three source classes: blazars, pulsars, and unassociated sources. The variability index quantifies the temporal variability of the source, and the curvature significance quantifies the spectral fit improvement between a power law and a log parabola (LP). The LP model (Zheng et al. 2023) is described by,

$$\frac{dN}{dE} = N_0 \left( \frac{E}{E_b} \right)^{-\left[ \alpha + \beta \log\left( \frac{E}{E_b} \right) \right]}, \quad (1)$$

where  $N_0$  is the normalization constant,  $E_b$  is the pivot energy (MeV),  $\alpha$  is the photon index at the pivot energy, and  $\beta$  is the curvature parameter. The peak energy<sup>2</sup> is given by  $E_{\text{peak}} = E_b \exp[(2 - \alpha)/(2\beta)]$ . We made use of data from the first version of the Fermi Large Area Telescope 14-year Source Catalog (`gll.psc.v32`). We also plot the unassociated Fermi source, 4FGL J0031.5–5648, on the figures with a magenta triangle.

There are several possible multiwavelength counterparts that lie within the Swift LSXPS and EP/FXT error regions. The Gaia counterpart, Gaia EDR3 4918773190794845824, has source coordinates R.A. = 7:89783331(7), DEC. = -56:77818634(7) and a proper motion consistent with zero, where PMRA =  $0.2 \pm 0.3$  mas/yr and PMDEC =  $-0.07 \pm 0.33$  mas/yr. The eROSITA counterpart was pointed out by Liu et al. (2024), with R.A. = 7:8973(4), DEC. = -56:7772(5) and IAU name 1eRASS J003135.3–564638 (Merloni et al. 2024). We also identified an infrared counterpart with source coordinates R.A. = 7:89771(6), DEC. = -56:77815(6), which is listed in the Wide-field Infrared Survey Explorer (WISE; Wright et al. 2010) All-Sky Source Catalog from the WISE satellite (WISE Team 2020), which surveyed the mid-infrared sky once in the four bands centered on 3.4, 4.6, 12, and 22  $\mu\text{m}$ . The catalog listed significant measurements for the first three bands, with magnitudes  $W_1 = 15.38(4)$ ,  $W_2 = 15.14(9)$ , and  $W_3 = 12.6(4)$ , respectively. We can thus determine WISE colors that will aid in classifying the source, where  $W_{12} := W_1 - W_2 = 0.24(10)$  and  $W_{23} := W_2 - W_3 = 2.6(4)$ .

### 4. DISCUSSION

We suggest that EP240709A is likely an active blazar from several independent pieces of information:

<sup>1</sup> [https://heasarc.gsfc.nasa.gov/docs/nicer/analysis\\_threads/background/](https://heasarc.gsfc.nasa.gov/docs/nicer/analysis_threads/background/)

<sup>2</sup> <https://docs.gammapy.org/0.7/api/gammapy.spectrum.models.LogParabola.html>

- The X-ray spectral and flux variability as shown in Figures 1 a), b), and c) are consistent with that of AGN (Mushotzky et al. 1993; McHardy 2010).
- The diagnostics shown in Figures 1 d) and e) show that 4FGL J0031.5–5648 is more likely to be a blazar compared to a pulsar, as it has a lower curvature significance, lower curvature parameter, and higher peak energy than pulsars in general.
- The machine-learning classification for the Gaia Data Release 3 (Gaia DR3) data set labeled a 99.98% probability for the source to be a quasar, determined through the Gaia Discrete Source Classifier utilizing Gaussian mixture models (Delchambre et al. 2023). We could not find any spectra from the Gaia archive.
- The two WISE colors are consistent with the infrared counterpart being a blazar, based on the  $W_1$ - $W_2$ - $W_3$   $\mu\text{m}$  color-color diagram of WISE thermal sources and blazars (Massaro et al. 2011; D’Abrusco et al. 2019). The counterpart could also be a high-frequency-peaked BL Lac (Massaro et al. 2011). Stellar systems tend to have redder  $W_1$ - $W_2$  (below 0.0) and  $W_2$ - $W_3$  (below 1.0) colors (D’Abrusco et al. 2019).

We note that given the large error circle of 4FGL J0031.5–5648 of roughly  $4'$  in the Fermi catalog, the counterparts identified above could simply be spatially coincident.

*Facilities:* NICER, eROSITA<sup>3</sup>, Swift, Gaia, Fermi, WISE<sup>4</sup>

*Software:* Astropy (Astropy Collaboration et al. 2013, 2018), NumPy and SciPy (Virtanen et al. 2020), Matplotlib (Hunter 2007), IPython (Perez & Granger 2007), HEASoft 6.33<sup>5</sup> (NASA High Energy Astrophysics Science Archive Research Center (HEASARC) 2014)

<sup>1</sup> Due to the word limit, we truncate the acknowledgements and link to the full text. This research has made use of data and/or software provided by HEASARC<sup>5</sup>. This work is based on data from eROSITA, the soft X-ray instrument aboard SRG<sup>3</sup>, and from the Wide-field Infrared Survey Explorer<sup>4</sup>. M.N. is a Fonds de Recherche du Quebec – Nature et Technologies (FRQNT) <sup>4</sup> postdoctoral fellow.

## REFERENCES

- Astropy Collaboration, Price-Whelan, A. M., et al. 2018, *AJ*, 156, 123, doi: [10.3847/1538-3881/aabc4f](https://doi.org/10.3847/1538-3881/aabc4f)
- Astropy Collaboration, Robitaille, T. P., et al. 2013, *A&A*, 558, A33, doi: [10.1051/0004-6361/201322068](https://doi.org/10.1051/0004-6361/201322068)
- D’Abrusco, R., et al. 2019, *ApJS*, 242, 4, doi: [10.3847/1538-4365/ab16f4](https://doi.org/10.3847/1538-4365/ab16f4)
- Delchambre, L., et al. 2023, *A&A*, 674, A31, doi: [10.1051/0004-6361/202243423](https://doi.org/10.1051/0004-6361/202243423)
- Evans, P. A., et al. 2023, *MNRAS*, 518, 174, doi: [10.1093/mnras/stac2937](https://doi.org/10.1093/mnras/stac2937)
- Folkner, W. M., et al. 2009, *Interplanetary Network Progress Report*, 42-178, 1
- Hunter, J. D. 2007, *Computing in Science and Engineering*, 9, 90, doi: [10.1109/MCSE.2007.55](https://doi.org/10.1109/MCSE.2007.55)
- Kaastra, J. S., & Bleeker, J. A. M. 2016, *A&A*, 587, A151, doi: [10.1051/0004-6361/201527395](https://doi.org/10.1051/0004-6361/201527395)
- Liu, M. J., et al. 2024, *The Astronomer’s Telegram*, 16704, 1
- Massaro, F., et al. 2011, *ApJL*, 740, L48, doi: [10.1088/2041-8205/740/2/L48](https://doi.org/10.1088/2041-8205/740/2/L48)
- McHardy, I. 2010, in *Lecture Notes in Physics*, Berlin Springer Verlag, ed. T. Belloni, Vol. 794, 203, doi: [10.1007/978-3-540-76937-8\\_8](https://doi.org/10.1007/978-3-540-76937-8_8)
- Merloni, A., et al. 2024, *A&A*, 682, A34, doi: [10.1051/0004-6361/202347165](https://doi.org/10.1051/0004-6361/202347165)
- Mushotzky, R. F., et al. 1993, *ARA&A*, 31, 717, doi: [10.1146/annurev.aa.31.090193.00344110.1146/annurev.astro.31.1.717](https://doi.org/10.1146/annurev.aa.31.090193.00344110.1146/annurev.astro.31.1.717)
- NASA High Energy Astrophysics Science Archive Research Center (HEASARC). 2014, HEASoft: Unified Release of FTOOLS and XANADU, Astrophysics Source Code Library, record ascl:1408.004. <http://ascl.net/1408.004>
- Papitto, A., & de Martino, D. 2022, in *Astrophysics and Space Science Library*, Vol. 465, Astrophysics and Space Science Library, ed. S. Bhattacharyya, A. Papitto, & D. Bhattacharya, 157–200, doi: [10.1007/978-3-030-85198-9\\_6](https://doi.org/10.1007/978-3-030-85198-9_6)
- Perez, F., & Granger, B. E. 2007, *Computing in Science and Engineering*, 9, 21, doi: [10.1109/MCSE.2007.53](https://doi.org/10.1109/MCSE.2007.53)
- Ransom, S. M., et al. 2002, *AJ*, 124, 1788, doi: [10.1086/342285](https://doi.org/10.1086/342285)
- <sup>3</sup> [https://erosita.mpe.mpg.de/dr1/AllSkySurveyData\\_dr1/acknowledgement.html](https://erosita.mpe.mpg.de/dr1/AllSkySurveyData_dr1/acknowledgement.html)
- <sup>4</sup> [https://wise2.ipac.caltech.edu/docs/release/allsky/expsup/sec1\\_6b.html](https://wise2.ipac.caltech.edu/docs/release/allsky/expsup/sec1_6b.html)
- <sup>5</sup> <https://heasarc.gsfc.nasa.gov/docs/heasarc/acknow.html>

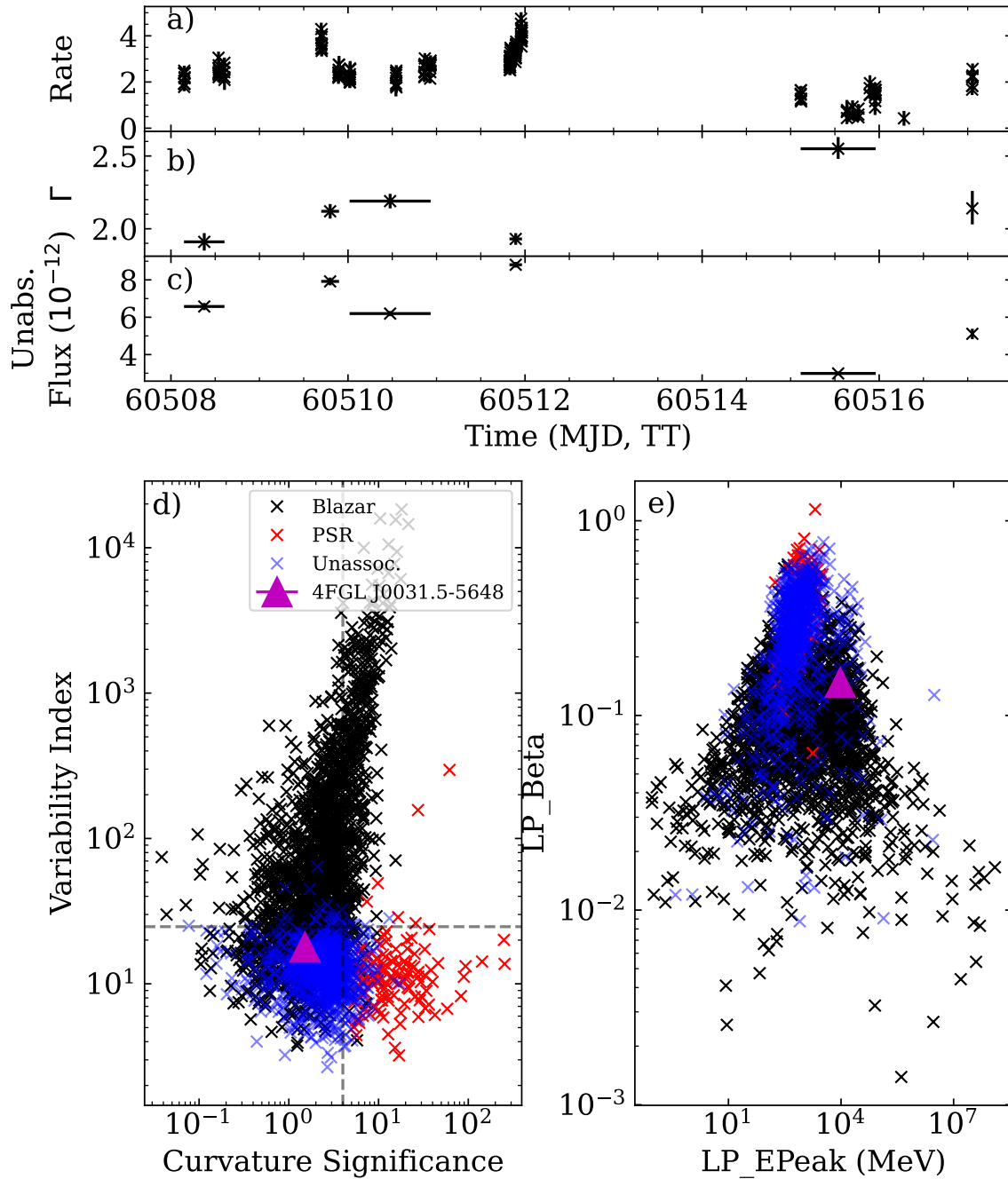


**Figure 1.** a) 0.4–3.0 keV background-subtracted NICER light curve (64 s bins); b) Power law photon index; and c) 0.3–10.0 keV unabsorbed flux in units of  $10^{-12} \text{ erg s}^{-1} \text{ cm}^{-2}$ . d) variability index vs. curvature significance; and e) curvature parameter and peak energy (in MeV).

Remillard, R. A., et al. 2022, *AJ*, 163, 130,

doi: [10.3847/1538-3881/ac4ae6](https://doi.org/10.3847/1538-3881/ac4ae6)

Vaughan, B. A., et al. 1994, *ApJ*, 435, 362, doi: [10.1086/174818](https://doi.org/10.1086/174818)

Virtanen, P., et al. 2020, *Nature Methods*, 17, 261,

doi: [10.1038/s41592-019-0686-2](https://doi.org/10.1038/s41592-019-0686-2)

WISE Team. 2020, *WISE All-Sky Source Catalog*, IPAC,

doi: [10.26131/IRSA142](https://doi.org/10.26131/IRSA142)

Wright, E. L., et al. 2010, *AJ*, 140, 1868,

doi: [10.1088/0004-6256/140/6/1868](https://doi.org/10.1088/0004-6256/140/6/1868)

Yuan, W., et al. 2022, in *Handbook of X-ray and Gamma-ray*

*Astrophysics*, ed. C. Bambi & A. Sanganello, 86,

doi: [10.1007/978-981-16-4544-0\\_151-1](https://doi.org/10.1007/978-981-16-4544-0_151-1)

Zheng, D., et al. 2023, *ApJ*, 952, 158,

doi: [10.3847/1538-4357/ace10b](https://doi.org/10.3847/1538-4357/ace10b)